Transcriptomic Signatures of Chicken DF-1 Cells Following Toll-Like Receptor 3 Stimulation

JeongWoong Park[1, †], Jae-Wan Jung[2, †], Andrew Wange Bugenyi[1, 3], Marc Ndimukaga[1], Anh Duc Truong[4], Jae Rung So[1], Nguyen Thu Uyen[1], Hoon Jang[2], Ki-Duk Song[1,5,*]

[1]Department of Agricultural Convergence Technology, Jeonbuk National University, Jeonju 54896, Republic of Korea

[2]Department of Life Sciences, Jeonbuk National University, Jeonju 54896, Republic of Korea

[3]National Agricultural Research Organization, Entebbe 295, Uganda

[4]Vietnam National Institute of Veterinary Research, Ha Noi, Vietnam

[5]International Agricultural Cooperation and Development Center, Jeonbuk National University, Jeonju 54896, Republic of Korea

[*]Corresponding author

Ki-Duk Song, Ph.D., Professor

Department of Agricultural Convergence Technology

Jeonbuk National University, Jeonju, Korea

Email: kiduk.song@jbnu.ac.kr; Tel.: +82-63-219-5523

[†]These authors contributed equally to this work

ORCID

JeongWoong Park: 0000-0003-0885-3078

Jae-Wan Jung: 0000-0002-2708-0704

Andrew Wange Bugenyi: 0000-0001-9036-8391

Marc Ndimukaga : 0000-0001-8061-7753

Anh Duc Truong: 0000-0002-2472-8165

Jae Rung So: 0000-0001-6786-6894

Nguyen Thu Uyen: 0009-0007-1295-5778

Hoon Jang: 0000-0001-8875-6854

Ki-Duk Song: 0000-0003-2827-0873

Running title: TLR3-Mediated Transcriptomic Response in Chicken DF-1 Cells

Abstract

Prophylactic agents and adjuvants induce immune responses against pathogens in animals, including chickens. Polyinosinic-polycytidylic acid (PIC), one of the prophylactic agents and a TLR3 agonist, mimics double-stranded viral RNA and triggers antiviral immune responses. This study employed RNA sequencing to analyze the transcriptional profile of DF-1 cells stimulated with PIC. Among 16,550 transcripts, 376 differentially expressed genes (DEGs) were identified, with 279 (74.2%) upregulated and 97 (25.8%) downregulated. Notably, PIC significantly increased the expression of inflammatory genes, particularly Interleukin 8-like 1 (IL8L1) (9.5-fold change), while downregulating Mitogen-activated protein kinase kinase 6 (MAP2K6). Gene Ontology analysis revealed enrichment of immune-related biological process (BP) terms, and REACTOME analysis highlighted significantly enriched pathways, including cytokine signaling in the immune system and regulation of the ERK1/2 and MAPK cascades. Dual-specificity phosphatases (DUSPs) and sprouty proteins (SPRYs), key regulators of ERK1/2 and MAPK signaling pathways, showed distinct upregulation upon PIC treatment, as confirmed by quantitative RT-PCR (qRT-PCR). Additionally, ERK and MAPK were upregulated in samples infected with Avian Influenza Virus (AIV), suggesting similarities in signaling pathways involved in viral immunity. These findings underscore the potential role of ERK1/2 and MAPK signaling pathways in mediating innate immune responses to PIC treatment and AIV infection, with DUSPs and SPRYs likely playing regulatory roles in these pathways. This study provides insight that could inform the development of antiviral and anticancer therapies.

Keywords: RNA sequencing, DF-1 cell, Toll-like receptor 3, MAPK pathways

1. Introduction

Viral diseases and other health conditions have been significant challenges to the poultry industry for a long time, affecting billions of birds and causing substantial economic losses worldwide [1, 2]. Strategies to mitigate these impacts include surveillance, quarantine of infected animals, and vaccine development. More recently, the stimulation of innate host responses using polyinosinic-polycytidylic acid (PIC) has emerged as a promising approach, as it induces the production of pro-inflammatory cytokines and enhances host antiviral responses. This strategy has shown effectiveness against viruses such as Newcastle disease virus (NCDV), Marek's disease virus (MDV), infectious bursal disease virus (IBDV), and low pathogenic avian influenza virus (LPAIV) [3, 4].

PIC is a synthetic analogue of double-stranded RNA, which is one of the pathogen-associated molecular patterns (PAMPs) that are recognized by a host's immune system through pattern recognition receptors (PRRs) [5-7]. Thus, PIC can mimic infection by dsRNA viruses and induce the host's defense response. One of the PRRs involved in the recognition of viral dsRNA is the toll-like receptor 3 (TLR3). In chicken, TLR3 is widely expressed in both immune cells, such as macrophages and myeloid dendritic cells (mDCs), and non-immune cells, such as fibroblasts, neurons, and epithelial cells [8-11]. It has been detected abundantly in chicken embryo fibroblasts (CEFs), chicken kidney cells (CKCs), DT-40, a chicken B cell-like cell line, and HD-11, a macrophage-like cell line. Similar to mammalian TLR3, chicken TLR3 recognizes dsRNA and its analog PIC, triggering the induction of type I interferons [12].

The DF-1 cell line, a chicken embryo fibroblast line, is an immortalized line derived from chicken embryo fibroblasts [13] and is widely used as a reliable in vitro model for studying avian viral infections, including those caused by Avian Influenza Virus (AIV) and Newcastle Disease Virus (NDV). Notably, the absence of endogenous retroviruses provides a clean experimental background for analyzing host-virus interactions. Therefore, elucidating the innate immune response pathways, such as TLR3-mediated signaling, in this well-established cell line is crucial for understanding early-stage cellular defense mechanisms in chickens. This knowledge can serve as a baseline for developing broad-spectrum antiviral strategies and for informing subsequent in vivo investigations.

Despite the known antiviral effects of PIC, there is limited information regarding the transcriptional profiles of DF-1 cells upon PIC stimulation. Previous studies evaluating PIC-induced responses in chicken cells have mainly relied on targeted qRT-PCR assays that examined only a small subset of cytokine- or interferon-related genes without providing genome-wide or pathway-level insights [13, 14]. An earlier transcriptomic analysis identified only 47 DEGs and provided limited interpretation of immune pathways, underscoring the need for broader genome-wide profiling [15]. Another study identified 714 DEGs but, similarly, lacked mechanistic insight into MAPK-associated regulators [16]. Our previous study also confirmed cytokine induction but was constrained by its targeted-gene approach, failing to reveal downstream regulatory components [13]. These limitations collectively highlight the necessity of comprehensive RNA-seq analysis to uncover regulatory modulators operating beyond classical cytokine pathways.

The MAPK signaling pathway plays a pivotal role in cellular responses, including

proliferation, differentiation, and immune regulation, making it a key target in host-pathogen interactions. To maintain proper cellular function, MAPK activity must be tightly regulated by various modulators, including phosphatases and feedback inhibitors. Among these, dual-specificity phosphatases (DUSPs) and Sprouty (SPRY) proteins serve as essential regulators of MAPK signaling. DUSPs act as negative regulators by dephosphorylating MAPKs, thereby controlling the activation of ERK, JNK, and p38 pathways, while SPRY proteins primarily inhibit the RAF-MEK-ERK cascade by interfering with receptor tyrosine kinase signaling [17-19].

In our previous work (Jang & Song, 2020) [13], we assessed PIC-induced innate immune responses in DF-1 cells using a limited qRT-PCR gene panel, confirming the induction of several pro-inflammatory and antiviral genes. However, that study did not investigate transcriptome-wide regulatory changes or explore MAPK-associated modulators such as DUSPs and SPRYs. The present study builds upon and significantly extends those earlier findings by employing RNA-seq to provide an unbiased analysis of global transcriptional responses to PIC, enabling the identification of previously uncharacterized regulatory pathways.

Given the central role of MAPK signaling in immune regulation, we investigated how PIC stimulation modulates the expression of key regulators, including DUSPs and SPRYs, in DF-1 cells. RNA sequencing (RNA-seq) analysis was performed to identify differentially expressed genes (DEGs) associated with these pathways. Additionally, selected DEGs were validated through quantitative RT-PCR (qRT-PCR). This research provides foundational insights critical for developing innovative strategies to prevent and treat viral diseases in poultry.

2. Materials and Methods

2.1. Cell culture and regulation of TLR signaling

DF-1 cells, a spontaneously immortalized continuous cell line derived from an East Lansing Line 0 (ev-0), were routinely cultured in high glucose Dulbecco's Modified Eagle's Medium (HG-DMEM) supplemented with 10% Fetal Calf Serum (FCS) at 37℃ in a 5% CO_2 incubator. To induce TLR signaling, the cells were washed once with phosphate-buffered saline (PBS), and treated with PIC at a concentration of 5μg/ml, followed by incubation for 6 hours. BAY 11–7085 (BAY), an NF-κB transcription factor inhibitor, was purchased from Sigma-Aldrich (St. Louis, MO, USA). SB203580 (p38 inhibitor), SP600125 (JNK inhibitor), and PD98059 (MEK inhibitor) were purchased from InvivoGen and MedChem Express (Monmouth Junction, NJ, USA), respectively. For NF-κB inhibition, DF-1 cells were treated with 5 μM BAY 11–7085 for 3 h before treatment with 5 μg/mL PIC. MEK inhibition was performed by treating DF-1 cells with 10 μM PD98059 (MEK inhibitor) for 18 h, followed by 6 h of stimulation with 5 μg/mL PIC. DF-1 cells were treated with 10 μM SB203580 for 1 h to disconnect the p38 MAPK pathway, followed by 6 h of stimulation with 5 μg/mL PIC. JNK inhibition was achieved by treating DF-1 cells with 25 μM SP600125 for 1 h, followed by stimulation for 6 h with 5 μg/mL PIC.

2.2. In vivo validation using the HPAIV infection model in chickens

To validate and compare the key signaling pathways identified from our in vitro DF-1 cell experiments, an *in vivo* infection model was utilized. A/chicken/Vietnam/NA-01/2019 (H5N1), a highly pathogenic avian influenza virus (HPAIV), was used in these experiments [18]. The viral isolate was propagated in 10-day-old embryonated chicken eggs at 37°C for 48 hours. The allantoic fluid (AF) was harvested from eggs, aliquoted, and stored at −80°C until use, in accordance with OIE guidelines (Chapter 3.3.4). The 50% infectious dose of eggs (EID50) of the influenza virus was determined as previously described [20]. Briefly, serial 10-fold dilutions of the virus were prepared in PBS, and 100 µl of each dilution was inoculated into the chorioallantoic cavities of 10-day-old embryonated chicken eggs. Five eggs were inoculated with each virus dilution and incubated at 37°C for 96 hours. The harvested AF was tested for haemagglutination (HA) activity using 0.5% red blood cells (RBC) according to the OIE guidelines (Chapter 3.3.4). The EID_{50}/mL of the virus suspension was calculated using the Reed-Muench method.

Specific pathogen-free (SPF) White Leghorn chickens (4 weeks old) were obtained from the Poultry Research Centre of the National Institute of Animal Science, Vietnam. Fifteen chickens per group were intranasally inoculated with 10^4 EID50 of A/chicken/Vietnam/NA-01/2019 (H5N1) in 200 µL AF. The control group consisted of 15 uninfected SPF White Leghorn chickens. Following viral infection, the chickens were monitored for clinical signs of disease. Samples were collected from the trachea on days 1, 2, and 3 post-infection, following the World Health Organization Manual on Animal Influenza Diagnosis and Surveillance [21]. All experiments were conducted in compliance with institutional guidelines for the care and use of laboratory animals, and the protocol was approved by the Ministry of Agriculture and Rural Development of Vietnam (TCVN 8402:2010 and TCVN 8400-26:2014).

2.3. RNA sequencing of PIC-stimulated DF-1 cells

Total RNA from the DF-1 cells was isolated from DF-1 cells in the presence or absence of PIC (3 mock-treated DF-1 cell samples, 3 PIC-treated DF-1 cell samples) using the TRIzol (Invitrogen, USA) reagent according to the manufacturer's instructions. RNA quality and integrity were assessed prior to library preparation. The TruSeq RNA Sample Prep Kit (Illumina) was used according to the manufacturer's guidelines for RNA sequencing. Human UHR total RNA (Agilent Technologies) was used as a technical positive control to verify that RNA extraction, library preparation, and sequencing were performed properly. This technical control served only to verify performance and was not used for biological comparison with DF-1 cells in this study. The library was constructed according to a standard Illumina, Inc. protocol. Libraries with different indexes were pooled and sequenced in a single lane on an Illumina HiSeq. 2000 high-throughput sequencing instrument with 100 paired-end (PE) reads.

2.4. Identification of Differentially Expressed Genes

The reads were processed using tools in the Galaxy public web server [22]. First, the reads were quality checked using FastQC (v0.74+galaxy0; [23]) and MultiQC (v1.11+galaxy1; [24]). High quality reads were then mapped to the latest chicken reference genome at the

time, bGalGal1.mat.broiler.GRCg7b (Ensembl; [25]), using RNA STAR (v2.7.11a+galaxy0; [26]). Gene-level quantification was done using featureCounts (Galaxy v2.0.3+galaxy2; [27]).

Gene counts were normalized and their differential expression analyzed using DESeq2 (Galaxy v2.11.40.8+galaxy0; [28]). Wald tests were applied to estimate statistical significance, and genes were considered differentially expressed when the FDR-adjusted p-value was <0.05 and the absolute log2 fold change was ≥2. Annotation of DEGs was performed using the Galaxy "Annotate DESeq2/DEXSeq output tables" tool (Galaxy v1.1.0), referencing the "bGalGal1.mat.broiler.GRCg7b" genome to assign gene symbols, biotypes, and other attributes. Visualization of DEG profiles was achieved through volcano plots generated with ggplot2 R package [29].

2.5. Bioinformatic analysis

Enriched Gene Ontology (GO) terms were identified using the R packages AnnotationDbi (version 1.68.0) [26] and GO.db (version 3.20.0) with a significance threshold of raw $p < 1.00\times 10^{-3}$ [30]. Additionally, a functional clustering analysis specific to the ERK1/2 and MAPK signaling pathways was conducted using DAVID, a web-based bioinformatics tool. The amino acid sequences of DUSPs and SPRYs from various vertebrate species were obtained Ensembl (release 62) genome browser (https://www.ensembl.org). Multiple sequence alignments were performed using the MUSCLE tool (http://www.ebi.ac.uk/Tools/msa/muscle/). Phylogenetic analysis was conducted using the Neighbor-Joining method with pairwise deletion, 1,000 bootstrap replications, and the Kimura 2- 2-parameter model, as described previously [31-33]. Functional enrichment and pathway analysis were conducted to identify the most functional annotations for significant genes using the g:Profiler tool [34]. In addition, the REACTOME database of pathways and reactions was used to visualize pathways in a directed acyclic hierarchy [35].

2.6. Quantitative Real-Time Polymerase Chain Reaction (qRT-PCR) of Differentially Expressed Genes

The nucleotide sequences of chicken candidate genes were retrieved from the National Center for Biotechnology Information (http://www.ncbi.nlm.nih.gov) and the Ensembl Genome Browser. Primers for gene amplification (Table 1) were designed using PRIMER3 software (http://bioinfo.ut.ee/primer3-0.4.0/). For validation of DEG expression, quantitative real-time PCR (RT-qPCR) was performed using SYBR Green Supermix on a CFX96™ IVD Real-time PCR System (Bio-Rad, Hercules, CA, USA). The primer sequences for the DEGs are listed in Table 1. The PCR conditions were as follows: an initial step at 94°C for 3 minutes, 39 cycles at 94°C for 10 seconds, 60°C for 30 seconds, and 72°C for 30 seconds, followed by a final step at 72°C for 10 minutes. Dissociation was performed at 0.5°C increments from 55°C to 95°C for over 25 minutes. Relative quantification analysis was performed using the comparative Ct ($2^{(-\Delta\Delta CT)}$) method [29-30]. *Glyceraldehyde-3-phosphate dehydrogenase* (*GAPDH*) was used as an endogenous control to detect mRNA levels.

2.7. Statistical analysis

Statistical analyses of qRT-PCR data were performed using GraphPad Prism. Comparisons between two groups were conducted using a two-tailed Student's t-test. For comparisons involving more than two groups, one-way analysis of variance (ANOVA) followed by Tukey's multiple comparison post hoc test was used. All data are presented as the mean ± standard error of the mean (SEM) from at least three independent biological replicates. A p-value of < 0.05 was considered statistically significant.

3. Results

3.1. Identification of DEGs induced by PIC treatment in DF-1 cells.

To investigate the transcriptomic responses induced by TLR3 signal activation through PIC treatment, high-throughput RNA sequencing analysis was performed on PIC-treated DF-1 cells (Supplementary Table S1). The sequencing data identified 16,550 transcripts, of which 279 were upregulated and 97 downregulated, as determined by scatter and volcano plots (Figure 1). DEGs were further classified according to their expression patterns (Supplementary Table S2). These results showed that the stimulation of DF-1 cells with PIC significantly increased the expression of several inflammation-related genes, including *Interleukin 8-like 1* (*IL8L1*) (205.5-fold change), *Interleukin 8-like 2* (*IL8L2*) (333.34 -fold change), *Chemokine (C-C motif) ligand 4* (*CCL4*) (73.7-fold change) and *Colony stimulating factor 3* (*CSF3*) (73.99-fold change), *Bradykinin receptor B1* (*BDKRB1*) (38.85-fold change) and the *Tumor necrosis factor superfamily member 15* (*TNFSF15*) (56.80-fold change). Conversely, *Mitogen-activated protein kinase kinase 6* (*MAP2K6*) showed the greatest decrease in expression (-15.79-fold).

3.2. Bioinformatics analysis of DEGs

Based on mRNA sequencing data, DEGs were annotated using the gene ontology in DF-1 cells after PIC treatment (Figure 2). The most significantly enriched GO terms included several Biological Process (BP) terms related to cell signal transduction, molecular function (MF) terms related to cytokine activity and inflammation, and cellular component (CC) terms associated with extracellular structure. For Kyoto Encyclopedia of Genes and Genomes (KEGG) pathways analysis, most of the enriched pathways identified were innate immune response related, including 'positive regulation of interleukin-2 production', 'positive regulation of transcription from RNA polymerase II promoter', influenza A, 'positive regulation of fibroblast proliferation', and 'regulation of apoptotic process' (Figure 2). As a result of activating biological process GO terms related to signal transduction and cell communication, we investigated the ERK1/2 and MAPK signaling pathways, which play roles in the innate host response. We identified 22 ERK1/2- and MAPK-signaling-related genes involved in innate host response (Table 2). A heatmap of these 22 genes shows a distinct expression signature that clearly separates PIC-treated samples from control samples (Supplementary Figure S1). Given that these GO terms highlight the regulation of critical immune signaling cascades, we focused our subsequent analysis on key regulatory gene families identified within these terms. Specifically, the Dual-specificity phosphatases (DUSPs) and Sprouty (SPRYs) families, known as crucial negative feedback regulators of MAPK and ERK signaling, were selected for further investigation to understand their role

in modulating the host response to PIC.

3.3. Functional annotation of immune response-related DEGs

To understand the immune response in DF-1 cells by PIC stimulation, enriched functional terms related to immune system processes were analyzed using Reactome. A total of 28 GO terms were identified and grouped into three main clusters from Reactome analysis (Supplementary Table S2).

The first cluster, associated with the adaptive immune system, included 8 GO terms such as T-cell receptor (TCR) signaling, co-stimulation by CD28 family, signaling by the B-cell receptor (BCR), class I MHC mediated antigen processing and presentation, MHC class II antigen presentation, immune-regulatory interactions between Lymphoid and non-Lymphoid cells, Rap 1 signaling, and Butyrophilin (BTN) family interactions.

The second cluster, related to innate immune system, a network of 14 GO terms comprised of TLR cascades, the complement cascade, nucleotide-binding domain leucine-rich repeat-containing receptor (NLR) signaling pathways, advanced glycosylation end-product receptor signaling, DDX58/IFIH1-mediated induction of interferon-alpha/beta, cytosolic sensors of pathogen-associated DNA, Fc-gamma receptor (FcγR)-dependent phagocytosis, DAP12 interactions, Fc-epsilon receptor (FcεR) signaling, C-type lectin receptors (CLRs), antimicrobial peptides, neutrophil degranulation, reactive oxygen species (ROS) and reactive nitrogen species (RNS) production in phagocytes, and the alpha-protein kinase 1 signaling pathway.

The final cluster, focused on cytokine signaling in the immune system, included a network of 6 GO terms: interferon signaling, interleukin signaling, growth hormone receptor signaling, prolactin receptor signaling, the TNFR2 non-canonical NF-κB pathway, and FLT3 signaling (Figure 3).

3.4. Evolutionary analysis and string analysis of innate host response-related differentially expressed genes

To investigate the evolutionary relationships of innate host response-related candidate DEGs, we extracted and compared amino acid sequences from eight vertebrate species (Rat, Mouse, Chicken, Human, Chimpanzee, Dog, Pig, and Cow). This analysis focused on two candidate gene families, DUSPs and SPRYs, which are RTK Signaling Antagonists.

Multiple sequence alignments of DUSPs and SPRYs revealed that the DSP_MAPKp domain and DUP_DUSPs domain in DUSPs (Supplementary Figure S2), as well as the Sprouty protein domain in SPRYs, exhibited high sequence identity (Supplementary Figure S3) across the analyzed species. The high conservation of these domains suggests they play essential, evolutionarily conserved roles in immune regulation.

3.5. Validation of DEGs in PIC-stimulated DF-1 Cells

When DF-1 cells were treated with PIC, apoptosis occurred gradually (Figure 4A). As established in our previous study [13], the PIC treatment system reliably induces immune responses. In this study, we confirmed the upregulation of immune-related genes such as *IL8L2*, *IL1β*, *IFNα*, and *IFNβ* under PIC treatment conditions (Figure 4B), further validating

the robustness of this system.

We used qRT-PCR to analyze changes in mRNA expression of MAPK14 (p38), MAPK8 (JNK), and MAPK3 (ERK1), representative components of the MAPK and ERK1/2 signaling pathways, in PIC-treated DF-1 cells (Figure 5). While the expression levels of *MAPK14* and *MAPK8* were not significantly altered, *MAPK*3 expression exhibited a significant increase (Figure 5A). These results suggest that ERK1/2 signaling plays a primary role in the innate immune response induced by PIC in DF-1 cells.

To further investigate downstream targets, we analyzed the expression of *DUSP* and *SPRY* genes, which regulate MAPK and ERK1/2 cascades. PIC treatment significantly upregulated the expression of *DUSP1*, *DUSP5*, DUSP8, and *SPRY4* (p<0.0001), as well as *DUSP6*, *SPRY1*, and *SPRY2*, compared to the control group (Figure 5B). These findings indicate that PIC strongly induces genes associated with ERK1/2 regulation.

To examine the role of p38 signaling in regulating *DUSP* and *SPRY* gene expression, DF-1 cells were treated with SB203580 (a p38 inhibitor), alongside PIC or PIC+SB203580 (Figure 5C). Comparisons between the PIC and PIC+SB203580 groups revealed no significant differences in *DUSP1*, *DUSP5*, or *DUSP8* expression. However, *DUSP6*, *SPRY2*, and *SPRY4* expression levels were significantly higher in the PIC group compared to the PIC+SB203580 group, while *SPRY1* expression exhibited an even greater difference. These results suggest that p38 signaling partially regulates specific DUSP and SPRY genes, but its overall contribution to the innate immune response in PIC-treated DF-1 cells appear limited.

To assess MEK signaling involvement, DF-1 cells were treated with PD98059 (a MEK inhibitor), either alone or in combination with PIC or PIC+PD98059 (Figure 5D). The PIC group exhibited significantly higher expression levels of DUSP5, SPRY1, and SPRY4 compared to the PIC+PD98059 group. Interestingly, SPRY1 expression was significantly higher in the PIC+PD98059 group than in the PIC group. This finding suggests that MEK signaling has a complex regulatory role, potentially mediating feedback inhibition or other compensatory mechanisms in response to PIC treatment.

To investigate NF-κB signaling, DF-1 cells were treated with BAY11-7085 (an NF-κB inhibitor), in combination with PIC or PIC+BAY11-7085 (Figure 5E). Comparisons between the PIC and PIC+BAY11-7085 groups showed no significant differences in *DUSP1* or *SPRY4* expression. However, *DUSP8* expression was significantly higher in the PIC group than in the PIC+BAY11-7085 group. In contrast, *DUSP5* and *SPRY1* expression levels were significantly higher in the PIC+BAY11-7085 group, while *DUSP6* and *SPRY2* expression levels were significantly higher in the PIC group. These results indicate that NF-κB signaling differentially regulates specific DUSP and SPRY genes in response to PIC.

3.6. QRT- PCR analysis of MAPKs genes and selected DUSPs and SPRYs genes in the trachea of HPAIV-infected chickens

To investigate the innate host response in vivo, we performed qRT-PCR using samples from white leghorn chickens infected with highly pathogenic avian influenza viruses (HPAIV) at different time points. The expression levels of *MAPK3* (*ERK1*), *MAPK8* (*JNK*), and *MAPK14* (*p38*) were significantly upregulated (Figure 6A), indicating that p38, JNK, and ERK signaling pathways are modulated by AI virus infection.

Additionally, as observed in qRT-PCR experiments conducted with PIC-treated DF-1 cells, DUSP expression was upregulated by influenza virus infection, whereas SPRY expression was downregulated (Figure 6B, C). Based on these findings, we propose that the innate host response mediated by DUSPs through the ERK and MAPK signaling pathways is influenced by influenza virus infection, while SPRYs may act as negative regulators during AIV infection.

4. Discussion

This study provides new insights into how PIC treatment influences the expression of MAPK/ERK pathway–associated regulatory molecules during an avian innate immune response.

Viral diseases are a serious threat to global health and present a major challenge to the poultry industry worldwide [1]. Numerous studies have demonstrated that immunostimulants can activate the immune system, especially the innate immune response, against various pathogens, including viruses [36-38]. One such stimulant, PIC, has been shown to induce antiviral and inflammatory responses [39], and has proven effective against various viral diseases, including NCDV, MDV, IBDV, AIV, Chikungunya virus, and others [3, 4, 40, 41]. In this study, we aimed to identify DEGs in DF-1 cells under PIC stimulation and to investigate the functional categories overrepresented among these DEGs. Additionally, we investigated which signaling pathway regulates the identified DEGs and functional categories. The DF-1 cell line, used in this study, is a suitable model for viral infection studies as it supports the proliferation of avian viruses, including AIV and NDV [15]. Although the number of DEGs identified in our study (376 DEGs) were fewer than in a related study by Yu et al. (714 DEGs) [16], they were significantly higher than the 47 DEGs identified in Kim and Zhou[15]. Importantly, 25 and 22 DEGS overlapped with these studies, respectively. Furthermore, compared with our previous work using targeted qRT-PCR analysis (Jang & Song, 2020) [13], the present study provides a transcriptome-wide investigation that reveals broader regulatory patterns not detectable using limited gene panels. This distinction clarifies how our study extends earlier findings and adds mechanistic depth to PIC-induced immune responses.

The highly upregulated chemokines and cytokines (*IL-8*, *CCL4*, *CSF3* and *TNFSF15*) suggest that PIC induced a coordinated pro-inflammatory response in DF-1 cells, consistent with established roles of these genes in immune cell recruitment and activation [42-48]. Functional enrichment analysis (Supplementary Table S3) further showed that these cytokine-and chemokine-associated DEGs clustered into biological categories related to chemotaxis, cytokine activity, and receptor–ligand interaction networks, reflecting broad activation of innate immune signaling pathways. Previous studies have reported the chemotactic role of cytokines after viral infection [49, 50]. Taken together, these findings indicate that PIC activates a coordinated inflammatory program characterized by chemotaxis and cytokine-driven signaling.

However, the mechanisms by which chemokine IL-8 recruits immune cells are not well understood [51]. TNFSF15 was particularly associated with apoptotic-related processes,

including regulation of apoptosis, programmed cell death, and overall cell death. Previous studies have shown that apoptosis is one of the antiviral innate immune mechanisms that organisms use to defend against viral infections [52, 53]. Thus, the induction of TNFSF15-linked apoptotic pathways may complement chemotactic inflammation as part of the PIC-triggered antiviral response.

On the other hand, *Mitogen-activated protein kinase kinase 6* (*MAP2K6*) expression was strongly downregulated, and subsequently, the MAPK pathway reaction was negatively regulated (Supplementary Table S3). MAP2K6 plays a key role in the p38 MAP kinase signal cascade that regulates several stimuli, including pro-inflammatory cytokines, bacterial lipopolysaccharides, UV, heat shock, or osmotic stress [54]. In PIC-induced DF-1 cells, this downregulation may have been a strategy to halt cell proliferation in a Raf (MAPKKK)-MEK (MAPKK)-ERK (MAPK) pathway [55], with negative regulation potentially mediated by upregulation of DUSP1, DUSP5, and DUSP8 [56]. While the exact mechanisms require further study, this observation aligns with previous findings on MAPK pathway regulation.

Interestingly, DEGs in the MAPK and ERK1/2 cascades were identified in our study. Among these DEGs, DUSP family genes and SPRY family genes were selected for validation. We validated that DUSPs and SPRYs were up-regulated in PIC-treated DF-1 cells. DUSPs are known to regulate MAPK signaling pathways, which are critical for controlling inflammatory and immune responses, while SPRYs act as RTK signaling antagonists and influence downstream MAPK activation. Given that PIC mimics viral dsRNA and activates antiviral signaling through TLR3, the induction of DUSPs and SPRYs more likely reflects their downstream roles in fine-tuning the magnitude and duration of MAPK signaling. This regulatory behavior is consistent with the evolutionary conservation of functional domains in DUSPs and SPRYs, which underscores their importance in innate immune regulation. Notably, these domains may play a crucial role in modulating the innate immune response upon PIC stimulation, as indicated by their evolutionary preservation and established functional relevance. This regulatory behavior is consistent with the established functional importance of conserved domains in DUSPs and SPRYs in innate immune regulation.

While earlier studies, including our previous qRT-PCR-based work [13], mainly focused on cytokine induction following PIC stimulation, the transcriptome-wide patterns observed here indicate additional regulatory features involving DUSPs and SPRYs. These molecules function as feedback modulators of MAPK signaling, suggesting that PIC triggers not only the well-characterized cytokine response but also engages fine-tuning circuits shaping the amplitude and duration of immune activation.

Many previous studies have reported that DUSPs are upregulated via ERK signaling, which is mediated by TLR [57, 58]. Similarly, we validated the upregulation of SPRY family genes in PIC-treated DF-1 cells. These DUSPs and SPRYs have been shown to have immune-related functions, including suppression of inflammatory cytokines, regulation of inflammatory gene expression, control of inflammation via JNK MAPKs, and regulation of T-cell survival in various studies [59-63]. Taken together, these findings support a role for DUSPs and SPRYs as key modulators of innate immune signalling. In addition, known

cross-talk among MAPK, NF-κB, and IRF pathways suggests that DUSP- and SPRY-mediated feedback may influence not only MAPK amplitude but also the timing of antiviral signaling responses. Although this was not directly tested here, our transcriptomic data support such an integrated regulatory model.

To further explore this regulatory architecture suggested by the transcriptomic data, expression patterns of DUSP and SPRY family genes were analyzed through MEK, P38, and JNK inhibitors to determine which signaling systems are regulated by DUSPs and SPRYs. Overall, DUSPs and SPRYs did not appear to be significantly affected by inhibitors. However, we observed that *DUSP6* was slightly down-regulated by P38 inhibitor treatment, and *SPRY2* and *SPRY4* were down-regulated under the same condition. Similarly, *DUSP5* and *SPRY4* were downregulated by the MEK inhibitor, whereas *DUSP6*, *DUSP8*, and *SPRY2* were reduced following the NF-κB inhibitor treatment. These differential responses suggest that DUSPs and SPRYs are not regulated by a single linear pathway, but rather are influenced by multiple signaling inputs downstream of PIC stimulation. This is consistent with the notion that their expression is shaped primarily by upstream TLR–MKK3/6 signaling rather than by direct inhibition of individual MAPK components [57, 64]. in line with previous studies, SPRY, like DUSPs, is known to be regulated by ERK signaling via MKK3/6 [65, 66]. Moreover, SPRYs have been reported to downregulate the expression of RAF, which in turn downregulates MEK expression by playing a role as a negative regulator [66, 67]. Collectively, these observations support the interpretation that DUSPs and SPRYs participate in higher-order feedback regulation of MAPK signaling rather than acting as simple downstream effectors.

Based on these findings, we confirmed the experimental results in the HPAIV samples, showing DUSPs were upregulated while SPRYs were downregulated in HPAIV-infected samples. This suggests that DUSPs and SPRYs are not merely genes regulated by the TLR signaling pathway; during virus infection, they are also regulated by MEK activity. In other words, PIC and AI infection share overlapping signaling pathways. It should be noted that for *in vivo* validation, we used tracheal tissue, a heterogeneous mixture of cell types, in contrast to the DF-1 fibroblast cell line used in our *in vitro* part of the study. This difference has implications for the transcriptomic profiles observed during comparisons. Nonetheless, within these considerations, valuable insights can be obtained. During AIV infection, it is plausible that SPRYs, as negative regulators, downregulate their expression to enhance ERK expression. These in vivo observations likely reflect context-dependent modulation of MAPK signaling rather than a direct mechanistic consequence of individual pathway components.

Therefore, the AIV dataset should be interpreted as supportive, rather than mechanistic, evidence. The in vivo expression patterns validate that several regulatory signatures observed in DF-1 cells also occur during natural infection, but they do not establish direct causal relationships. Thus, the AIV findings primarily provide translational reinforcement of our transcriptomic observations, complementing but not defining the mechanistic interpretation derived from the in vitro data. In this context, the present study provides significant insights into the transcriptomic response of chicken cells to TLR3 stimulation.

5. Conclusions

Overall, this study provided additional information on PIC-induced immune responses and their regulation in DF-1 cells and in Avian influenza-infected samples. The findings suggest that PIC stimulates a strong pro-inflammatory response in DF-1 cells and shed light on immune response genes and associated biological pathways not previously reported. Some candidate genes (DUSPs and SPRYs) were involved in both positive and negative regulation of innate immune response in various health conditions. Therefore, further studies should elucidate additional signaling pathways (e.g., MKK 3/6) that may regulate ERK1/2, DUSPs, and SPRYs. Additionally, the immune roles and anti-inflammatory activities of DUSPs and SPRYs should also be explored in the search for new therapeutics against various conditions.

Competing Interests

The authors report there are no competing interests to declare.

Acknowledgements

This work was supported by the Basic Science Research Program through the National Research Foundation of Korea (NRF), funded by the Ministry of Education (2021R1I1A3057071). J-W. J. was supported by Global-Learning & Academic research institution for Master's·PhD students and Postdocs (LAMP) Program of the National Research Foundation of Korea (NRF) grant funded by the Ministry of Education (No. RS-2024-00443714)

Contributions:

Conceptualization, K.D.S. and J.W.J.; methodology, J.W.P. and J.W.J.; validation, S.J.K.; formal analysis, J.W.P. and J.W.J.; investigation, J.R.S.; resources, A.D.T.; data curation, J.W.P., J.R.S, N.T.U.; writing—original draft preparation, J.W.P; writing—review and editing, K.D.S, J.W.J. and H.J.; visualization, A.W.B.; supervision, K.D.S.; project administration, K.D.S.; funding acquisition, K.D.S. All authors have read and agreed to the published version of the manuscript.

Ethics approval and consent to participate

All animal experiments were conducted in compliance with the institutional rules for the care and use of laboratory animals, as well as implementing the protocol approved by the Ministry of Agriculture and Rural Development of Vietnam (TCVN 8402:2010 and TCVN 8400-26:2014)

Data availability statement.

Authors agree to make data and materials supporting the results or analyses presented in their paper available upon reasonable request.

References

1. Jordan AB, Gongora V, Hartley D, Oura C. A Review of Eight High-Priority, Economically Important Viral Pathogens of Poultry within the Caribbean Region. Vet Sci. 2018;5(1) DOI: ARTN 14 10.3390/vetsci5010014.
2. Kim TH, Zhou HJ. Overexpression of Chicken IRF7 Increased Viral Replication and Programmed Cell Death to the Avian Influenza Virus Infection Through TGF-Beta/FoxO Signaling Axis in DF-1. Front Genet. 2018;9 DOI: ARTN 415 10.3389/fgene.2018.00415.
3. Ahmed-Hassan H, Abdul-Cader MS, De Silva Senapathi U, Sabry MA, Hamza E, Nagy E, et al. Potential mediators of in ovo delivered double stranded (ds) RNA-induced innate response against low pathogenic avian influenza virus infection. Virol J. 2018;15(1):43 DOI: 10.1186/s12985-018-0954-2.
4. He X, Chen Y, Kang S, Chen G, Wei P. Differential Regulation of chTLR3 by Infectious Bursal Disease Viruses with Different Virulence In Vitro and In Vivo. Viral Immunol. 2017;30(7):490-9 DOI: 10.1089/vim.2016.0134.
5. Bavananthasivam J, Kulkarni RR, Read L, Sharif S. Reduction of Marek's Disease Virus Infection by Toll-Like Receptor Ligands in Chicken Embryo Fibroblast Cells. Viral Immunol. 2018;31(5):389-96 DOI: 10.1089/vim.2017.0195.
6. Lundberg AM, Drexler SK, Monaco C, Williams LM, Sacre SM, Feldmann M, et al. Key differences in TLR3/poly I:C signaling and cytokine induction by human primary cells: a phenomenon absent from murine cell systems. Blood. 2007;110(9):3245-52 DOI: 10.1182/blood-2007-02-072934.
7. Tatematsu M, Nishikawa F, Seya T, Matsumoto M. Toll-like receptor 3 recognizes incomplete stem structures in single-stranded viral RNA. Nat Commun. 2013;4:1833 DOI: 10.1038/ncomms2857.
8. Akira S, Uematsu S, Takeuchi O. Pathogen recognition and innate immunity. Cell. 2006;124(4):783-801 DOI: 10.1016/j.cell.2006.02.015.
9. Medzhitov R, Janeway CA, Jr. Innate immunity: the virtues of a nonclonal system of recognition. Cell. 1997;91(3):295-8 DOI: 10.1016/s0092-8674(00)80412-2.
10. Kawai T, Akira S. The role of pattern-recognition receptors in innate immunity: update on Toll-like receptors. Nat Immunol. 2010;11(5):373-84 DOI: 10.1038/ni.1863.
11. Bugge M, Bergstrom B, Eide OK, Solli H, Kjonstad IF, Stenvik J, et al. Surface Toll-like receptor 3 expression in metastatic intestinal epithelial cells induces inflammatory cytokine production and promotes invasiveness. J Biol Chem. 2017;292(37):15408-25 DOI: 10.1074/jbc.M117.784090.
12. Chen S, Cheng A, Wang M. Innate sensing of viruses by pattern recognition receptors in birds. Vet Res. 2013;44(1):82 DOI: 10.1186/1297-9716-44-82.

13. Jang HJ, Song KD. Expression patterns of innate immunity-related genes in response to polyinosinic:polycytidylic acid (poly[I:C]) stimulation in DF-1 chicken fibroblast cells. J Anim Sci Technol. 2020;62(3):385-95 DOI: 10.5187/jast.2020.62.3.385.
14. Karpala AJ, Lowenthal JW, Bean AG. Activation of the TLR3 pathway regulates IFNβ production in chickens. Dev Comp Immunol. 2008;32(4):435-44 DOI: 10.1016/j.dci.2007.08.004.
15. Kim TH, Zhou HJ. Functional Analysis of Chicken IRF7 in Response to dsRNA Analog Poly(I:C) by Integrating Overexpression and Knockdown (vol 10, e0133450, 2015). Plos One. 2015;10(9) DOI: ARTN e0137672
10.1371/journal.pone.0137672.
16. Yu SM, Mao HY, Jin ML, Lin X. Transcriptomic Analysis of the Chicken MDA5 Response Genes. Genes-Basel. 2020;11(3) DOI: ARTN 308
10.3390/genes11030308.
17. Patterson KI, Brummer T, O'Brien PM, Daly RJ. Dual-specificity phosphatases: critical regulators with diverse cellular targets. Biochem J. 2009;418(3):475-89 DOI: 10.1042/bj20082234.
18. Mason JM, Morrison DJ, Basson MA, Licht JD. Sprouty proteins: multifaceted negative-feedback regulators of receptor tyrosine kinase signaling. Trends Cell Biol. 2006;16(1):45-54 DOI: 10.1016/j.tcb.2005.11.004.
19. Keyse SM. Dual-specificity MAP kinase phosphatases (MKPs) and cancer. Cancer Metastasis Rev. 2008;27(2):253-61 DOI: 10.1007/s10555-008-9123-1.
20. Huprikar J, Rabinowitz S. A simplified plaque assay for influenza viruses in Madin-Darby kidney (MDCK) cells. J Virol Methods. 1980;1(2):117-20 DOI: 10.1016/0166-0934(80)90020-8.
21. WHO. Cumulative number of confirmed human cases for avian influenza A(H5N1) reported to WHO, 2003-2024, 28 March 2024. 2024.
22. Afgan E, Baker D, Van den Beek M, Blankenberg D, Bouvier D, Čech M, et al. The Galaxy platform for accessible, reproducible and collaborative biomedical analyses: 2016 update. Nucleic acids research. 2016;44(W1):W3-W10 DOI: https://doi.org/10.1093/nar/gkw343.
23. Andrews S. FastQC: a quality control tool for high throughput sequence data. 2010. 2017 DOI: http://www.bioinformatics.babraham.ac.uk/projects/fastqc.
24. Ewels P, Magnusson M, Lundin S, Käller M. MultiQC: summarize analysis results for multiple tools and samples in a single report. Bioinformatics. 2016;32(19):3047-8 DOI: https://doi.org/10.1093/bioinformatics/btw354.
25. Harrison PW, Amode MR, Austine-Orimoloye O, Azov AG, Barba M, Barnes I, et al. Ensembl 2024. Nucleic acids research. 2024;52(D1):D891-D9 DOI: https://doi.org/10.1093/nar/gkad1049.
26. Dobin A, Davis CA, Schlesinger F, Drenkow J, Zaleski C, Jha S, et al. STAR: ultrafast universal RNA-seq aligner. Bioinformatics. 2013;29(1):15-21 DOI: https://doi.org/10.1093/bioinformatics/bts635.

27. Liao Y, Smyth GK, Shi W. featureCounts: an efficient general purpose program for assigning sequence reads to genomic features. Bioinformatics. 2014;30(7):923-30 DOI: https://doi.org/10.1093/bioinformatics/btt656.
28. Love MI, Huber W, Anders S. Moderated estimation of fold change and dispersion for RNA-seq data with DESeq2. Genome biology. 2014;15:1-21 DOI: https://doi.org/10.1186/s13059-014-0550-8.
29. Wickham H. ggplot2: Elegant Graphics for Data Analysis: Springer-Verlag New York; 2016.
30. Carlson M, Falcon S, Pages H, Li N. GO. db: A set of annotation maps describing the entire Gene Ontology. R package version. 2019;3(2):10.18129 DOI: https://doi.org/doi:10.18129/B9.bioc.GO.db.
31. Saitou N, Nei M. The neighbor-joining method: a new method for reconstructing phylogenetic trees. Mol Biol Evol. 1987;4(4):406-25 DOI: 10.1093/oxfordjournals.molbev.a040454.
32. Felsenstein J. Confidence Limits on Phylogenies: An Approach Using the Bootstrap. Evolution. 1985;39(4):783-91 DOI: 10.1111/j.1558-5646.1985.tb00420.x.
33. Kimura M. A Simple Method for Estimating Evolutionary Rates of Base Substitutions through Comparative Studies of Nucleotide-Sequences. J Mol Evol. 1980;16(2):111-20 DOI: Doi 10.1007/Bf01731581.
34. Raudvere U, Kolberg L, Kuzmin I, Arak T, Adler P, Peterson H, et al. g:Profiler: a web server for functional enrichment analysis and conversions of gene lists (2019 update). Nucleic Acids Res. 2019;47(W1):W191-W8 DOI: 10.1093/nar/gkz369.
35. Fabregat A, Jupe S, Matthews L, Sidiropoulos K, Gillespie M, Garapati P, et al. The Reactome Pathway Knowledgebase. Nucleic Acids Res. 2018;46(D1):D649-D55 DOI: 10.1093/nar/gkx1132.
36. Alvarez-Rodríguez M, Pereiro P, Reyes-López FE, Tort L, Figueras A, Novoa B. Analysis of the Long-Lived Responses Induced by Immunostimulants and Their Effects on a Viral Infection in Zebrafish (Danio rerio). Front Immunol. 2018;9 DOI: ARTN 1575 10.3389/fimmu.2018.01575.
37. Hackett CJ. Innate immune activation as a broad-spectrum biodefense strategy: Prospects and research challenges. J Allergy Clin Immun. 2003;112(4):686-94 DOI: 10.1016/S0091-6749(03)02025-6.
38. Lee HC, Lee ES, Uddin MB, Kim TH, Kim JH, Chathuranga K, et al. Released Tryptophanyl-tRNA Synthetase Stimulates Innate Immune Responses against Viral Infection. J Virol. 2019;93(2) DOI: ARTN e01291-18 10.1128/JVI.01291-18.
39. Das A, Chai JC, Kim SH, Lee YS, Park KS, Jung KH, et al. Transcriptome sequencing of microglial cells stimulated with TLR3 and TLR4 ligands. Bmc Genomics. 2015;16 DOI: ARTN 517 10.1186/s12864-015-1728-5.

40. Jin B, Sun T, Yu XH, Liu CQ, Yang YX, Lu P, et al. Immunomodulatory Effects of dsRNA and Its Potential as Vaccine Adjuvant. J Biomed Biotechnol. 2010 DOI: Artn 690438 10.1155/2010/690438.
41. Li YG, Siripanyaphinyo U, Tumkosit U, Noranate N, A-nuegoonpipat A, Pan Y, et al. Poly (I:C), an agonist of toll-like receptor-3, inhibits replication of the Chikungunya virus in BEAS-2B cells. Virology Journal. 2012;9 DOI: Artn 114 10.1186/1743-422x-9-114.
42. Chang TT, Chen JW. Emerging role of chemokine CC motif ligand 4 related mechanisms in diabetes mellitus and cardiovascular disease: friends or foes? Cardiovasc Diabetol. 2016;15(1):117 DOI: 10.1186/s12933-016-0439-9.
43. Meniailo ME, Malashchenko VV, Shmarov VA, Gazatova ND, Melashchenko OB, Goncharov AG, et al. Interleukin-8 favors pro-inflammatory activity of human monocytes/macrophages. Int Immunopharmacol. 2018;56:217-21 DOI: 10.1016/j.intimp.2018.01.036.
44. Liu YS, Hsu JW, Lin HY, Lai SW, Huang BR, Tsai CF, et al. Bradykinin B1 receptor contributes to interleukin-8 production and glioblastoma migration through interaction of STAT3 and SP-1. Neuropharmacology. 2019;144:143-54 DOI: 10.1016/j.neuropharm.2018.10.033.
45. Schneider A, Krüger C, Steigleder T, Weber D, Pitzer C, Laage R, et al. The hematopoietic factor G-CSF is a neuronal ligand that counteracts programmed cell death and drives neurogenesis. J Clin Invest. 2005;115(8):2083-98 DOI: 10.1172/Jci23559.
46. Gao H, Niu ZR, Zhang Z, Wu HJ, Xie YN, Yang ZB, et al. promoter polymorphisms increase the susceptibility to small cell lung cancer: a case-control study. Bmc Med Genet. 2019;20 DOI: ARTN 29 10.1186/s12881-019-0762-6.
47. Jin S, Chin J, Seeber S, Niewoehner J, Weiser B, Beaucamp N, et al. TL1A/TNFSF15 directly induces proinflammatory cytokines, including TNFα, from CD3+CD161+T cells to exacerbate gut inflammation. Mucosal Immunol. 2013;6(5):886-99 DOI: 10.1038/mi.2012.124.
48. Richard AC, Peters JE, Savinykh N, Lee JC, Hawley ET, Meylan F, et al. Reduced monocyte and macrophage TNFSF15/TL1A expression is associated with susceptibility to inflammatory bowel disease. Plos Genet. 2018;14(9) DOI: ARTN e1007458 10.1371/journal.pgen.1007458.
49. Karpala AJ, Stewart C, McKay J, Lowenthal JW, Bean AGD. Characterization of Chicken Mda5 Activity: Regulation of IFN-β in the Absence of RIG-I Functionality. J Immunol. 2011;186(9):5397-405 DOI: 10.4049/jimmunol.1003712.
50. Liniger M, Summerfield A, Zimmer G, McCullough KC, Ruggli N. Chicken Cells Sense Influenza A Virus Infection through MDA5 and CARDIF Signaling Involving LGP2. J Virol. 2012;86(2):705-17 DOI: 10.1128/Jvi.00742-11.

51. St Paul M, Paolucci S, Barjesteh N, Wood RD, Sharif S. Chicken erythrocytes respond to Toll-like receptor ligands by up-regulating cytokine transcripts. Res Vet Sci. 2013;95(1):87-91 DOI: 10.1016/j.rvsc.2013.01.024.
52. Lee S, Hirohama M, Noguchi M, Nagata K, Kawaguchi A. Influenza A Virus Infection Triggers Pyroptosis and Apoptosis of Respiratory Epithelial Cells through the Type I Interferon Signaling Pathway in a Mutually Exclusive Manner. J Virol. 2018;92(14) DOI: ARTN e00396-18 10.1128/JVI.00396-18.
53. Nainu F, Shiratsuchi A, Nakanishi Y. Induction of Apoptosis and Subsequent Phagocytosis of Virus-Infected Cells As an Antiviral Mechanism. Front Immunol. 2017;8 DOI: ARTN 1220 10.3389/fimmu.2017.01220.
54. Matsumoto T, Kinoshita T, Matsuzaka H, Nakai R, Kirii Y, Yokota K, et al. Crystal structure of non-phosphorylated MAP2K6 in a putative auto-inhibition state. J Biochem. 2012;151(5):541-9 DOI: 10.1093/jb/mvs023.
55. Iwasa H, Han JH, Ishikawa F. Mitogen-activated protein kinase p38 defines the common senescence-signalling pathway. Genes Cells. 2003;8(2):131-44 DOI: DOI 10.1046/j.1365-2443.2003.00620.x.
56. Lake D, Corrêa SAL, Müller J. Negative feedback regulation of the ERK1/2 MAPK pathway. Cell Mol Life Sci. 2016;73(23):4397-413 DOI: 10.1007/s00018-016-2297-8.
57. Lang R, Hammer M, Mages J. DUSP meet immunology: Dual specificity MAPK phosphatases in control of the inflammatory response. J Immunol. 2006;177(11):7497-504 DOI: DOI 10.4049/jimmunol.177.11.7497.
58. Huang CY, Tan TH. DUSPs, to MAP kinases and beyond. Cell Biosci. 2012;2 DOI: Artn 24 10.1186/2045-3701-2-24.
59. Hammer M, Echtenachter B, Weighardt H, Jozefowski K, Rose-John S, Männel DN, et al. Increased inflammation and lethality of Dusp1−/− mice in polymicrobial peritonitis models. Immunology. 2010;131(3):395-404 DOI: 10.1111/j.1365-2567.2010.03313.x.
60. Habibian JS, Jefic M, Bagchi RA, Lane RH, McKnight RA, McKinsey TA, et al. DUSP5 functions as a feedback regulator of TNFα-induced ERK1/2 dephosphorylation and inflammatory gene expression in adipocytes. Sci Rep-Uk. 2017;7 DOI: ARTN 12879 10.1038/s41598-017-12861-y.
61. Tögel L, Nightingale R, Wu R, Chüeh AC, Al-Obaidi S, Luk I, et al. is methylated in CIMP-high colorectal cancer but is not a major regulator of intestinal cell proliferation and tumorigenesis. Sci Rep-Uk. 2018;8 DOI: ARTN 1767 10.1038/s41598-018-20176-9.
62. Ding T, Zhou Y, Long RY, Chen C, Zhao JJ, Cui PP, et al. DUSP8 phosphatase: structure, functions, expression regulation and the role in human diseases. Cell Biosci. 2019;9(1) DOI: ARTN 70 10.1186/s13578-019-0329-4.

704 63. Shehata HM, Khan S, Chen E, Fields PE, Flavell RA, Sanjabi S. Lack of Sprouty 1 and 2
705 enhances survival of effector CD8
706 T cells and yields more protective memory cells. P Natl Acad Sci USA. 2018;115(38):E8939-E47
707 DOI: 10.1073/pnas.1808320115.
708 64. Manley GCA, Parker LC, Zhang YL. Emerging Regulatory Roles of Dual-Specificity
709 Phosphatases in Inflammatory Airway Disease. Int J Mol Sci. 2019;20(3) DOI: ARTN 678
710 10.3390/ijms20030678.
711 65. Ozaki K, Kadomoto R, Asato K, Tanimura S, Itoh N, Kohno M. ERK pathway positively
712 regulates the expression of Sprouty genes. Biochem Bioph Res Co. 2001;285(5):1084-8 DOI:
713 10.1006/bbrc.2001.5295.
714 66. Reich A, Sapir A, Shilo BZ. Sprouty is a general inhibitor of receptor tyrosine kinase
715 signaling. Development. 1999;126(18):4139-47.
716 67. Lo TL, Fong CW, Yusoff P, Mckie AB, Chua MS, Leung HY, et al. Sprouty and cancer: The
717 first terms report. Cancer Lett. 2006;242(2):141-50 DOI: 10.1016/j.canlet.2005.12.032.
718

719 **Table 1.** Primer sets used in this study

Primer name	Primer sequence (5′ to 3′)	Tm (°C)	Product size (bp)
IL8L2 F	CCAAGCACACCTCTCTTCCA	58	176
IL8L2 R	GCAAGGTAGGACGCTGGTAA	-	-
IL1b F	GGATTCTGAGCACACCACAGT	58	272
IL1b R	TCTGGTTGATGTCGAAGATGTC	-	-
IFNa F	GACAGCCAACGCCAAAGC	60	78
IFNa R	GTCGCTGCTGTCCAAGCATT	-	-
IFNb F	CCTCCAACACCTCTTCAACATG	60	69
IFNb R	TGGCGTGCGGTCAAT	-	-
MAPK14 F	CGTCTGTTCTGCCTTTGACA	60	218
MAPK14 R	CCATGAGGTGTGTCACCAAG	-	-
MAPK8 F	TGCCACAAAATCCTCTTTCC	60	230
MAPK8 R	TCCCTTGCTTGACTTGCTTT	-	-
MAPK3 F	CTGACCCCAAAGCACTTGAT	60	235
MAPK3 R	GATCGATATCCTGGCTGGAA	-	-
DUSP1 F	TTCCCAGTCTCCATCCCTGT	60	196
DUSP1 R	CTAGGACACGTGGATGGCTC	-	-
DUSP5 F	GAGCGATGTGGAGAGGAACC	60	144
DUSP5 R	AGGAACTCGCACTTGGAAGC	-	-
DUSP6 F	CTCCACGAATCTGGACGTTT	60	293
DUSP6 R	CATCGTTCATGGACAGGTTG	-	-
DUSP8 F	AGTCACTTCATGCGCATTCC	60	153
DUSP8 R	GATGGTGGCTGACCGGGATA	-	-
SPRY1 F	TTGAGCAGATCAACCAGCAC	60	245
SPRY1 R	CATTTGCACTTCCCACACTG	-	-
SPRY2 F	ATCATCTTCAGGGCCAGTTG	60	291
SPRY2 R	TTGTCCTCATCATCGTTGGA	-	-
SPRY4 F	GCACTTTCTGCTGTGCGAAG	60	
SPRY4 R	GGTGGAGTAGTTGACCAGGC	-	-
GAPDH F	TGCTGCCCAGAACATCATCC	60	142
GAPDH R	ACGGCAGGTCAGGTCAACAA	-	-

720

721 **Table 2.** Biological process gene ontology terms of MAPK and ERK 1 /2 cascade -related
722 differentially expressed genes in PIC treated DF-1 cells.

Term	RT	Count	P-Value	Gene list
GOTERM_ BP_DIRECT	negative regulation of ERK1 and ERK2 cascade	10	1.70E-03	ABL1, RANBP9, TIMP3, TNIP1, ATF3, DUSP6, SPRY1, SPRY2, SPRY4, SYNJ2BP
	positive regulation of MAPK cascade	11	2.50E-03	CD40, FAS, RELT, TNFRSF11B, ADRB2, AR, CDON, FGFR2, IGFBP3, IL11, PDGFB

723

Figure legends

(A) **(B)**

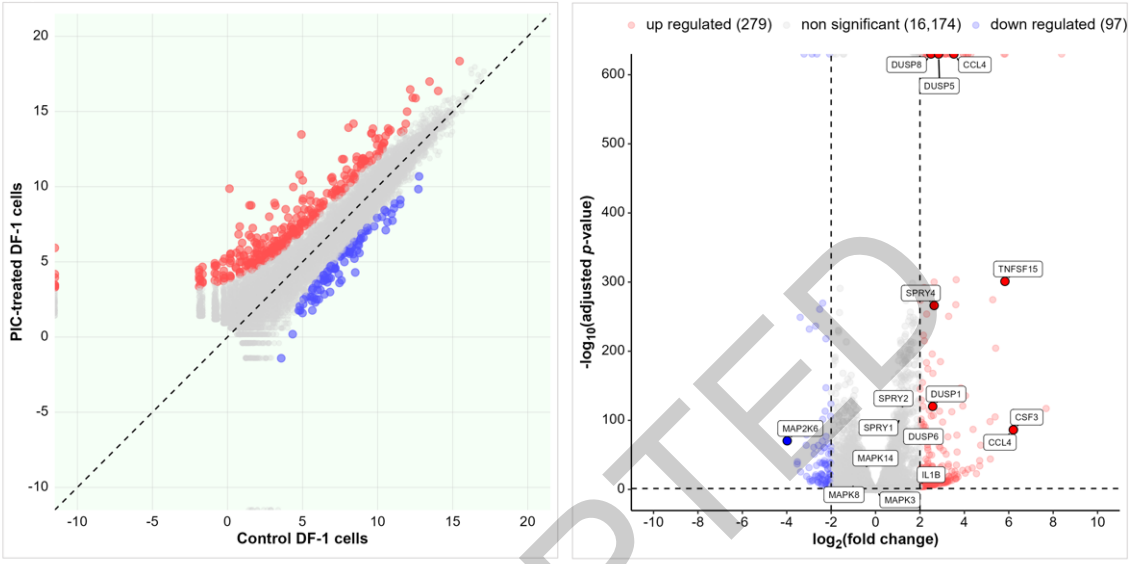

Figure 1. RNA- sequencing (NGS) data. (a) Scatter plot analysis showing DEGs between control and PIC-treated DF-1 cells. (b) Volcano plot analysis depicting DEGs between control and PIC-treated DF-1 cells. The color gradient from blue to red represents low to high gene expression levels. This figure provides an overview of the transcriptomic response to PIC stimulation, which serves as the basis for downstream pathway-level analyses, including MAPK/ERK-associated regulatory genes such as DUSPs and SPRYs.

Figure 2. Biological process gene ontology analysis of differentially expressed genes. These enriched biological processes include MAPK-associated immune responses, providing a functional framework for downstream validation of MAPK regulators such as DUSPs and SPRYs.

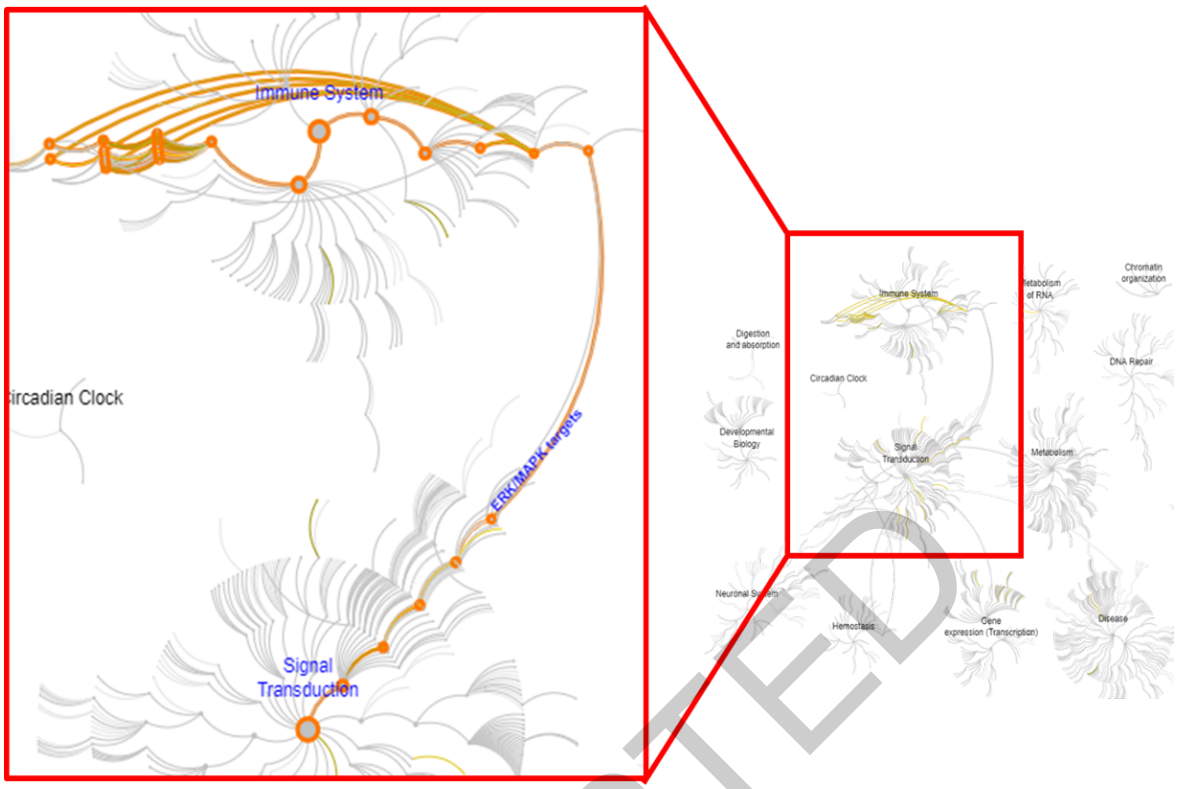

Figure 3. A genome-wide overview of pathway analysis. Reactome pathways are organized hierarchically. The center of each of the circular "bursts" represents the root of a top-level pathway. Each concentric step moving outward corresponds to the next lower level in the pathway hierarchy. Among the significantly enriched pathways were MAPK activation, cytokine signaling, and receptor-ligand interaction modules, which collectively support the pathway-level framework in which DUSP/SPRY-mediated feedback operates following PIC stimulation.

(A)

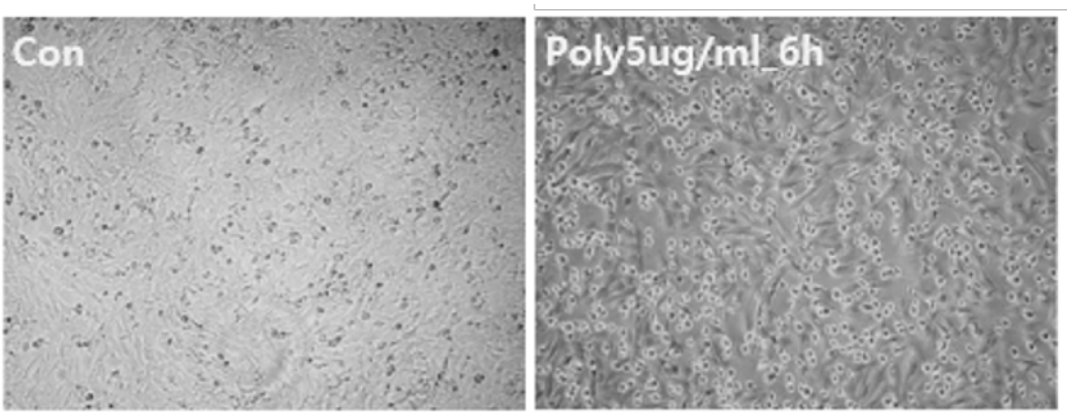

(B)

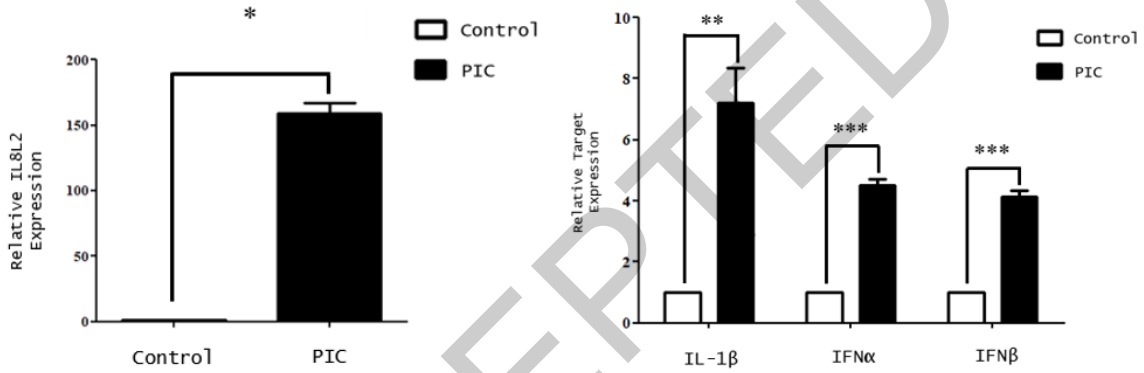

Figure 4. Comparative analysis between control and PIC-treated DF-1 cells. (A) Morphology of DF-1 cells by PIC treatment. (B) The expressions of IL8L2, IL1β, IFNα, and IFNβ in DF-1 cells by treatment with PIC (*p<0.05, n=3). Quantitative analysis was performed using the $2^{\wedge\text{-}\Delta\Delta Ct}$ method, normalized to *GAPDH*. These cytokine induction patterns confirm activation of innate antiviral signaling and provide upstream context for MAPK/ERK pathway engagement, which is later examined through DUSP/SPRY expression and inhibitor analyses.

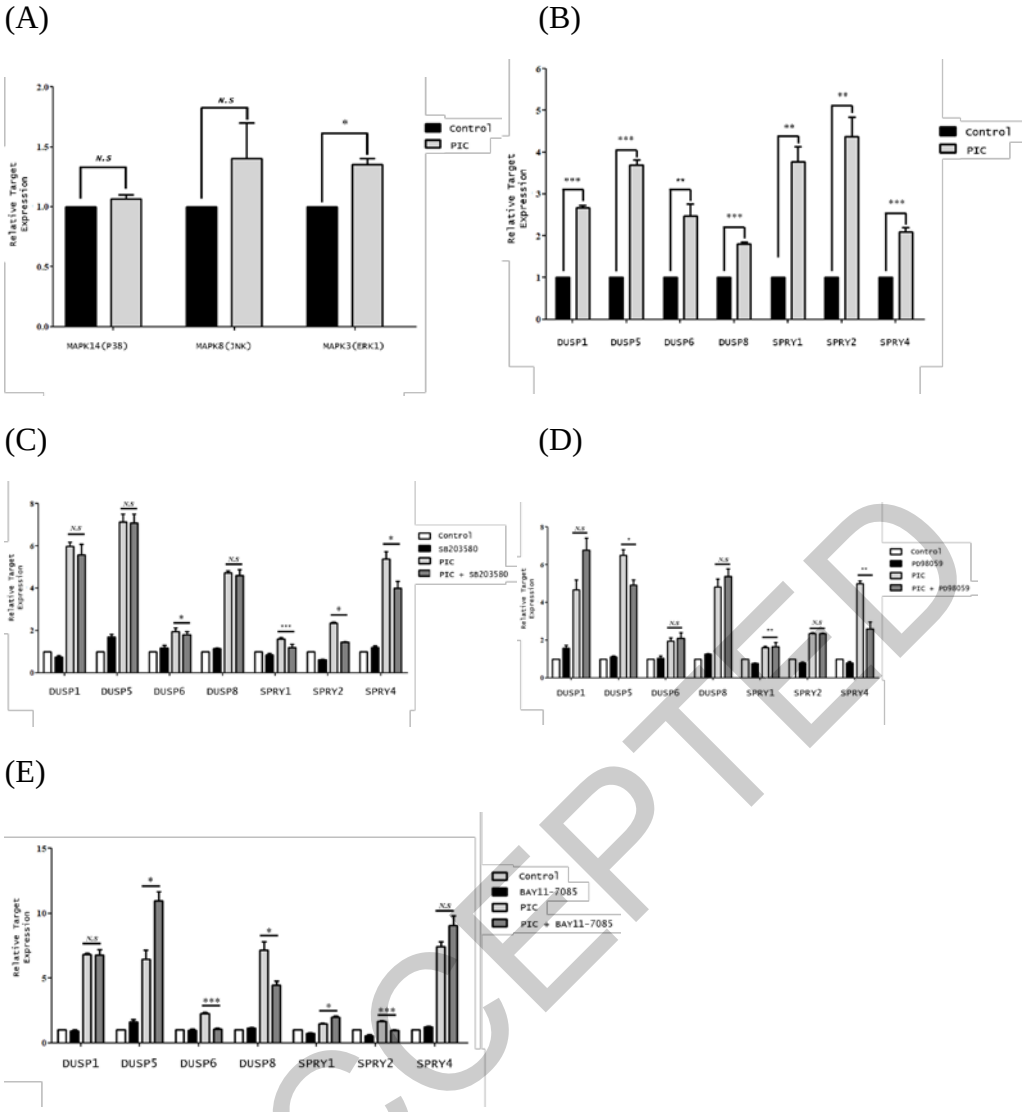

Figure 5. Effects of PIC Treatment and Pathway Inhibitors on MAPK and ERK1/2 Signaling-Related Gene Expression in DF-1 Cells. (A) Relative mRNA expression levels of *MAPK14* (*p38*), *MAPK8* (*JNK*), and *MAPK3* (*ERK1*) in PIC-treated DF-1 cells. (B) Relative mRNA expression levels of *DUSPs* (*DUSP1*, *DUSP5*, *DUSP6*, *DUSP8*) and *SPRY* (*SPRY1*, *SPRY2*, *SPRY4*) genes in response to PIC treatment. (C) Effects of SB203580 (a p38 inhibitor), (D) PD98059 (a MEK inhibitor), and (E) BAY11-7085 (an NF-κB inhibitor) on DUSP and SPRY gene expression in PIC-treated DF-1 cells. Relative expression levels were normalized to beta-actin expression and calculated using the $2^{-\Delta\Delta Ct}$ method. Data represent the mean ± SEM. Statistical significance was determined using t-tests or one-way ANOVA with post hoc tests (*p<0.01, **p<0.001 ***p<0.0001. N.S indicates no significance, n=3). This figure directly interrogates MAPK pathway regulation by evaluating DUSP/SPRY responses to PIC and pathway-specific inhibitors. These analyses highlight the roles of DUSPs and SPRYs as feedback modulators that fine-tune MAPK/ERK signaling rather than acting as primary cytokine drivers.

(A) (B)

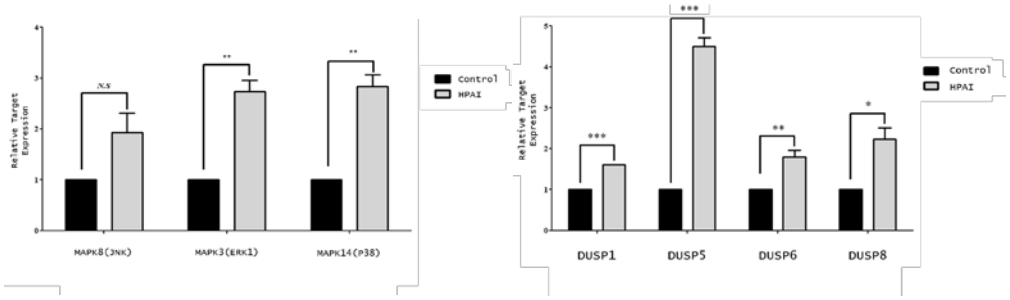

(C)

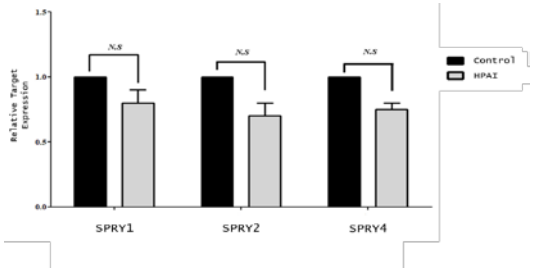

Figure 6. qRT-PCR validation of MAPK and selected *DUSPs and SPRYs* genes in trachea of highly pathogenic avian influenza-infected chickens. Expression levels of MAPKs, DUSP genes, and SPRY genes were analyzed by qRT-PCR (**p*<0.5, ***p*<0.01, ****p*<0.001, n=3). Quantitative analysis was performed using the 2−ΔΔCt method by normalization to beta-actin gene expression. The in vivo expression patterns mirror several DUSP/SPRY-associated regulatory features observed in vitro, providing supportive evidence that MAPK/ERK fine-tuning mechanisms identified in DF-1 cells also arise during natural viral infection, reinforcing their potential roles as modulators of antiviral signaling networks.